

Conventional and Advanced Exergetic and Exergoeconomic Analysis of an IRSOFC-GT-ORC Hybrid System

Shabnam Ghorbani ^{1,2}, Mohammad Hassan Khoshgoftar Manesh ^{1,2*}

¹ Division of Thermal Science & Energy Systems, Department of Mechanical Engineering, Faculty of Technology & Engineering, University of Qom, Qom, Iran

² Center of Environmental Research, University of Qom, Qom, Iran

Received: 2019-10-10

Revised: 2019-12-07

Accepted: 2019-12-14

Abstract: Due to the necessity of using highly efficient power generation systems to reduce fuel consumption and air pollution, the integration of different energy systems is promising modification to achieve higher efficiency. In this paper, the integration of an Internal Reforming Solid Oxide Fuel Cell (IRSOFC)-Gas Turbine (GT)-Organic Rankine Cycle (ORC) system has been proposed. In this regard, thermodynamic modeling and simulation of the proposed system have been done to evaluate the performance of the integrated system. Also, exergetic, exergoeconomic and advanced exergetic analysis has been performed for the proposed system. The analysis of the integrated system has been carried out by using MATLAB code. Verification of thermodynamic simulation has been performed with high accuracy. Results of thermodynamic simulation show that the net power and overall cycle efficiency of the proposed cycle are increased by 1.1 MW and 7.7 % respectively rather initial SOFC-GT combination. The exergy analysis indicated that exergy efficiency is 40.95%, for the proposed system and 37.3% for the initial base case. As a result, the exergy destruction, exergoeconomic factor, cost rate per exergy unit of product and fuel, and cost rate associated with the exergy destruction for each component are calculated and evaluated. Also, endogenous/exogenous and avoidable/unavoidable parts of exergy destruction, exergy destruction costs, and capital costs have been determined and compared.

keywords: Solid Oxide Fuel Cell, Gas Turbine, Organic Rankine Cycle, Exergy, Advanced Exergy Analysis

1. Introduction

Today increasing in consumption of fossil fuels, environmental and ecological problems, leads to find new and clean methods for power generation. Fuel Cell is one of the clean energy conversion devices for electricity generation. Among different types of fuel cells, SOFC and MCFC have good potential to employ in cogeneration systems due to their high working temperature (McPhail, Aarva, Devianto, Bove, & Moreno, 2011). High rate of electrochemical reactions, no need to costly metal catalyst, fuel flexibility without need external reforming, usability of high quality wasted heat of SOFCs in other thermal cycles are several advantages that lead to SOFCs be more cost-effective than other low-temperature fuel cells (Ni, Leung, & Leung, 2009). Chan et al. (Chan, Low, & Ding, 2002) studied two simple SOFC power systems fed by hydrogen

and methane respectively and showed that the system uses methane is more efficient than the system uses hydrogen as feedstock. Because of high working temperature and pressure, SOFCs can be the key candidate for integration with gas turbines (Shirazi, Aminyavari, Najafi, Rinaldi, & Razaghi, 2012). A literature survey shows the concept of using a gas turbine power plant with SOFC in an integrated system initially investigated by Ide et al (Sghaier, Khir, & Brahim, 2018). The strategies for SOFC-based integration systems are studied by Zhang et al (Zhang et al., 2010) and classified to direct coupling, indirect coupling, and fuel coupling. In direct thermal coupling, SOFC exhaust gases are directly fed to two or more power systems, in other word in direct-coupled SOFC-GT, the GT combustor is swapped by the stack of SOFC and SOFC-Brayton system share the same working fluid,

* Corresponding Author.

Authors' Email Address: ¹ Sh. Ghorbani (ghorbanishn@gmail.com), ² M. H. Khoshgoftar Manesh (mh.khoshgoftar@gmail.com)

ISSN (Online): 2345-4172, ISSN (Print): 2322-3251

© 2020 University of Isfahan. All rights reserved

while indirectly coupled SOFC-GT are operated with two different streams that thermally coupled through a heat exchanger. The heat addition of the gas cycle combustion chamber is supplemented by exhaust heat produced by the topping SOFC. The same method is applied in the semi-indirect coupling, but the GT exhaust stream is also directly fed to the SOFC cathode so this type of coupling can improve overall efficiency. Wang et al investigated a direct combination of the SOFC/GT system with the Kalina cycle to improve conversion efficiency (Wang, Yan, Ma, & Dai, 2012). Thermodynamic analysis of a Methane-fed internal reforming solid oxide fuel cell-gas turbine power generation system has been performed by Bavarsad [7]. The effect of fuel flow rate, airflow rate, temperature and pressure on system performance have been investigated and found that increasing the fuel flow rate does not have a satisfactory effect on system performance. A similar study on this subject, consist of a fuel cell power generation system fed by methane have analyzed by performance criteria coefficient (EPC) over the entire range of potential operating conditions by Akkaya et al. They concluded that EPC method gives a new basis for understanding engineering decisions (Akkaya et al., 2008). The literature review shows that many authors have more interest to study direct-coupled pressurized SOFC hybrid cycles. Using pressurized SOFC as combustors in gas turbine or steam turbine results to increase efficiency over 70% (Choudhury, Chandra, & Arora, 2013). Exergetic analysis of a new combined SOFC-GT cycle by Motahar et al shows that in the overall hybrid system, the combustion chamber and fuel cell stack have more share in exergy destruction (Motahar & Alemrajabi, 2009). A thermo-economic modeling of indirect (Cheddie & Murray, 2010b) and semi-direct (Cheddie & Murray, 2010a) coupling of SOFC/GT power plant studied by Cheddie et al. They concluded that these types of coupling significantly improves the second law performance of the system. An optimal thermo-economic analysis of four direct-coupled SOFC-GT with pressurized and atmospheric designs studied by Pirkandi et al. and showed that hybrid system with one pressurized fuel cell hybrid system is better than other (Pirkandi, Mahmoodi, & Ommian, 2017). Eveloy et al. also performed an exergoeconomic analysis of an indirect coupled IRSOFC-GT-ORC power system. The results show that for proposed system efficiency improvements of approximately 34% compared with the base GT cycle, and of 6% relative to the hybrid SOFC-GT sub-system.

A simulation and Performance analysis of the SOFC-Stirling engine based on simulation in Matlab and Modeling in Hysys have been performed by Ramezani et al (Ramezani, Amidpour, Najafi, & Abbaspour, 2015).

In order to reduce total energy consumption, Ahmadi et al used a combined cycle of SOFC and GT as thermal resources of multiple effect desalination systems (Ahmadi, Pourfatemi, Ghaffari, Muhammad, & Ghaffari, 2017).

In some other research, the integration of Molten Carbonate Fuel Cell has been considered. Exergoeconomic analysis of a combined Nitrogen rejection plant with LNG and NGL processes based on the MFC and Absorption cooling systems has been investigated (Ghorbani, Hamedi, & Amidpour, 2016). Furthermore, Ghorbani et al proposed an integrated trigeneration incorporating hybrid energy systems for natural gas liquefaction. Superstructure is including Molten Carbonate Fuel cell (MCFC), gas turbine, water-ammonia absorption refrigeration system (Ghorbani, Shirmohamadi, Mehrpoya, & Mafi 2018). In the other work, Ghorbani et al focused on the integration of the MCFC power plant and the multiple-effect desalination system (Ghorbani, Mehrpooya, & Mousavi, 2019). A literature survey shows that many researchers have been studied in the field of application of SOFCs and MCFCs in the CHP hybrid system and power generation section. Most of them investigated these systems in view of thermodynamic, exergetic and economic point. However, an advanced exergy analysis for a SOFC by the engineering and modified hybrid approaches has been performed by Fallah et al (Fallah, Mahmoudi, & Yari, 2018). They found that fewer endogenous exergy destructions are predicted by the engineering method. Rangei et al (Rangel-hernández et al., 2018) focused on advanced exergy analysis applied to a SOFC/vapor adsorption refrigeration (VAR) system. The effects of four main parameters (fuel temperature, fuel utilization, current density, and carbon-to-steam ratio) on the exergy efficiency of both stand-alone and integrated systems are investigated.

As shown in the literature review, only two recent studies have been done in the field of advanced exergetic analysis of SOFC and many studies focused on thermal, exergetic and exergoeconomic parametric analysis of SOFC-CHP systems. The first purpose of the present study is to study the effect of both coupling type i.e. a direct SOFC-GT that indirectly integrated with a topping Brayton cycle and bottoming ORC in a novel hybrid system, to enhance power generation capacity and efficiency. The

second purpose is to demonstrate the application of conventional and advanced exergetic analysis of this novel cogeneration system. In this regard, thermodynamic simulation of the proposed plant has been performed in MATLAB code with high accuracy. Also, this code calculated conventional and advanced exergetic and exergoeconomic analysis based on engineering approach.

2. System Description

The proposed system consists of an open Brayton cycle that indirectly coupled with a direct integrated SOFC-GT combined system and called the topping cycle. For this coupling, five SOFC stack is used. All data about one SOFC stack and other components are represented in Table (1). Due to the high thermal energy of exhaust gases this topping cycle integrated with an Organic Rankine Cycle by Heat Recovery Vapor Generator (HRVG). A simple schematic of the proposed system is shown in Fig. 1

2.1. Assumptions

The following assumptions are made to modeling and analysis system:

- The air mixture is considered as 21% oxygen and 79% nitrogen.
 - The fuel composition supplied to the system consists of 100% methane.
 - The system worked at steady-state conditions.
 - There is no gas leakage from the system.
 - Change in kinetic and potential energy is ignored.
 - The gas and air behave as an ideal gas.
 - Temperature, pressure, and chemical components distribution inside the cell is ignored.
 - Gasses that exiting the cathode and anode have the same temperature.
 - The fuel inside the fuel cell is processed into hydrogen via internal reforming(Pirkandi, Ghassemi, Hamedi, & Mohammadi, 2012).
- And for ORC:
- The system worked at a steady-state condition.
 - The working fluid at the turbine inlet and condenser outlet is saturated vapor and saturated liquid respectively.
 - The heat losses in the components of ORC are neglected.
 - The effects of all kinds of pipes and valves are neglected to simplify the system

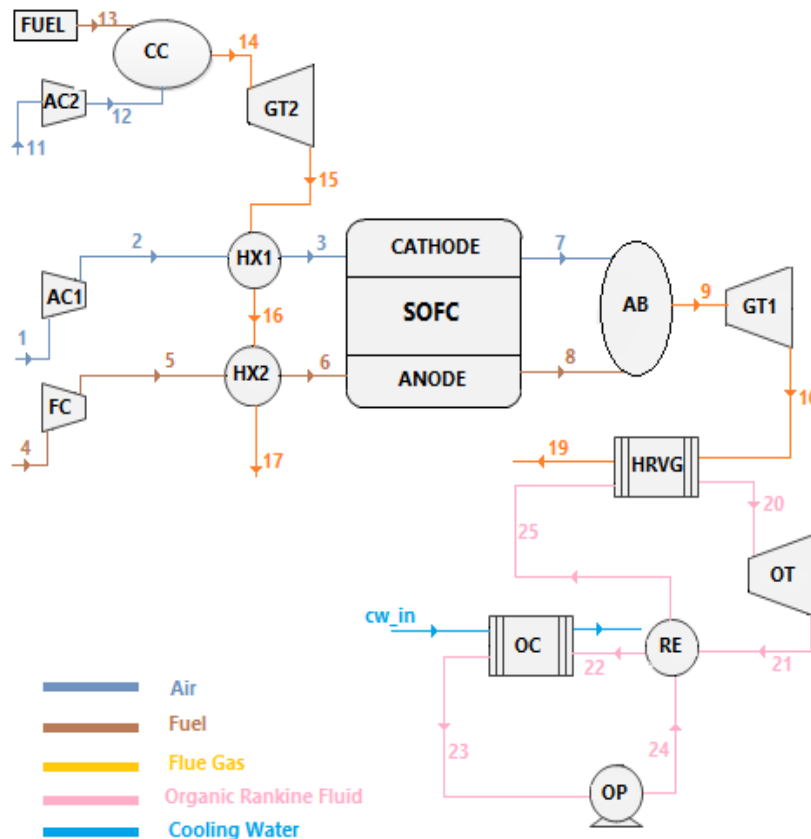
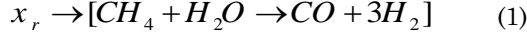


Figure 1. Schematic of the proposed hybrid system Schematic must be capital

3. The Governing Equations

3.1. Solid Oxide Fuel Cell

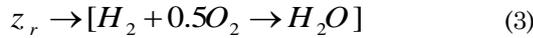
The electrochemical reactions that occur in SOFC lead to converting part of the chemical energy of the fuel into electrical energy. The following overall reactions occur in the SOFC anode (Eveloy, Karunkeyoon, Rodgers, & Al Aili, 2016). The steam reforming reaction is:



Shifting reaction:



And, the overall electrochemistry reaction is:



Where the x_r , y_r and z_r respectively denote molar conversion rates of progress in the cell reforming, shifting and electrochemistry reactions (Pirkandi et al., 2012).

Air utilization ratio and fuel utilization factor respectively defined as (Chitsaz, Mahmoudi, & Rosen, 2015):

$$U_{air} = \frac{(Air)_{consumed}}{(Air)_{supplied}} \quad (4)$$

$$U_f = \frac{(fuel)_{consumed}}{(fuel)_{supplied}} \quad (5)$$

The equilibrium constant of shifting reaction is defined as (Chitsaz et al., 2015):

$$\ln K_s = \ln \left[\frac{y_r(3x_r + y_r - z_r)}{(x_r - y_r)(1.5x_r - y_r + z_r)} \right] \quad (6)$$

SOFC current density depends on cell numbers and cell area and expressed as:

$$j = \frac{2.F.z_r}{N.A_{cell}} \quad (7)$$

And for one SOFC stack:

$$I = j.A_{cell} \quad (8)$$

$$W_{SOFC} = N.I.V_{cell} \quad (9)$$

Where E_r is maximum cell voltage and calculated from the Nernst equation (Bavarsad, 2007):

$$E_r = E^o + \frac{R_u T}{n_e F} \ln \left(\frac{P_{H_2} P_{O_2}^{1/2}}{P_{H_2O}} \right) \quad (10)$$

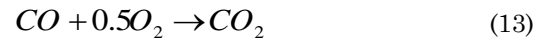
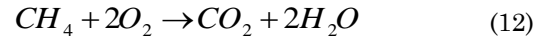
When electrons flow through the circuit the cell voltage decreases due to some losses. These losses called over potentials and classified into three types:(i) ohmic resistance; (ii) electrochemical reaction activation and (iii) concentration depletion (Bavarsad, 2007).

$$E = E_r - \eta_{ohm} - \eta_{con} - \eta_{act} \quad (11)$$

Detailed data about these overpotentials are presented in Table (2).

3.2. Combustion Chamber and After Burner

The following reactions occur in the combustion chamber (Eveloy, Rodgers, & Qiu, 2016):



Since the fuel cell output consists of steam, carbon monoxide, carbon dioxide, and hydrogen, to utilize the amount of air and fuel that not used in SOFC used an afterburner to increase the output flow temperature. The reactions that occur in afterburner are:



To find outflowing gasses temperature, following equations is used (Haseli, Dincer, & Naterer, 2008):

$$n_7 \bar{h}_7 + n_g \bar{h}_g - n_9 \bar{h}_9 - Q_{Loss,ab} = 0 \quad (16)$$

$$Q_{Loss,ab} = n_4 \times (1 - U_f) \times (1 - \eta_{ab}) \times LHV \quad (17)$$

That LHV represents the low heating value of fuel and $Q_{Loss,ab}$ is the amount of heat loss at the afterburner chamber.

3.3. Gas Turbine

The topping open Brayton cycle is a 5.2-MW gas turbine power plant with natural gas as fuel and turbine inlet temperature of 1450.15K, the pressure ratio of this cycle is 11. To calculate power generation by GT, outlet pressure and temperature in the gas turbine, by regarding isentropic efficiency the following relations are considered (Pirkandi et al., 2012):

$$\eta_{gt} = \frac{w_{gt,a}}{w_{gt,s}} = \frac{\overline{h_{in}} - \overline{h_{out}}}{\overline{h_{in}} - \overline{h_{out,s}}} = \frac{T_{in} - T_{out}}{T_{in} - T_{out,s}} \quad (18)$$

$$P_{out} = P_{in} \times \left(\frac{T_{out,s}}{T_{in}} \right)^{\frac{k_g}{k_g - 1}} \quad (19)$$

$$W_{gt} = m_{gas} \times (\overline{h_{in}} - \overline{h_{out}}) \quad (20)$$

3.4. Air and Fuel Compressors

The data about the compression ratio and isentropic efficiency presented in Table (1). For air compressor (Pirkandi et al., 2012):

$$\frac{T_{out,s}}{T_{in}} = \left(\frac{P_{out}}{P_{in}} \right)^{\frac{k_a - 1}{k_a}} = (r_p)^{\frac{k_a - 1}{k_a}} \quad (21)$$

$$\eta_{ac} = \frac{w_{ac,s}}{w_{ac}} = \frac{\overline{h_{out,s}} - \overline{h_{in}}}{\overline{h_{out}} - \overline{h_{in}}} = \frac{T_{out,s} - T_{in}}{T_{out} - T_{in}} \quad (22)$$

$$W_{ac} = m_{air} \times (\overline{h_{out}} - \overline{h_{in}}) \quad (23)$$

Fuel compressor calculations is similar to air compressors.

3.5. Heat Exchanger

To calculate outlet temperatures in heat exchangers by considering the efficiency of heat exchanger (Pirkandi et al., 2012) the following equation is used:

$$\varepsilon = \frac{Q}{Q_{max}} = \frac{m \times C_p \times \Delta T}{(m \times C_p)_{min} \times \Delta T_{max}} \quad (24)$$

Table 1. main design parameters for the proposed hybrid system

Main parameter	value	Main parameter	value
Fuel utilization factor	0.85	Turbine isentropic efficiency (%)	90
Pressure loss in fuelcell stack (%)	5	Brayton cycle air compressor efficiency (%)	85
Pressure loss in afterburner/Combustion Chamber (%)	5	Cell area (cm ²)	1036.2
Pressure loss in heat exchanger (%)	4	Length of each cell (cm)	150
Pressure loss in HRVG and recuperator (%)	5	Diameter of each cell (cm)	2.2
gas/air heat exchanger effectiveness (%)	85	Number of cells for one stack	5857
gas/fuel heat exchanger effectiveness (%)	85	Current density (A/m ²)	3000
Fuel and air compressor efficiency (%)	81	SOFC stack Temperature (K)	1273
Micro Turbine isentropic efficiency (%)	81	SOFC air and fuel Compression ratio	3.255
		Brayton cycle Compression ratio	11
		Turbine inlet temperature T _{14 in} (K)	1450.15

Table 2. Electrochemical equations for SOFC calculation

Main parameter	Value
Ohmic loss (Motahar et al., 2009)	$V_{ohm,an} = \frac{i \rho_{an} (A \pi d)^2}{8 \delta_{an}}$ $V_{ohm,ca} = \frac{i \rho_{ca} (\pi d)^2}{8 \delta_{ca}} A [A + 2(1 - A - B)]$ $V_{ohm,el} = i \rho \delta_{el}$
Activation polarization (Pirkandi et al., 2012)	$V_{ohm,in} = i (\pi d) \rho_{in} \frac{\delta_{in}}{\omega_{in}}$ $V_{act} = V_{act,an} + V_{act,ca}$ $V_{act} = \frac{2R_u T}{n_e F} \sinh^{-1} \left(\frac{i}{2i_0} \right)$
Concentration loss (Pirkandi et al., 2012)	$V_{conc,an} = \frac{R_u T}{n_e F} \ln \left(\frac{1 - i / i_{L,H_2}}{1 + i / i_{L,H_2O}} \right)$ $V_{conc,ca} = \frac{R_u T}{n_e F} \ln \left(\frac{1}{1 - i / i_{L,O_2}} \right)$

3.6. Organic Rankin Cycle

The Organic Rankine Cycle is one of the heat conversion technologies and is so useful to recover low-grade heat and the possibility to be implemented in decentralized lower-capacity power plants (Quoilin, Van Den Broek, Declaye, Dewallef, & Lemort, 2013). The selection of working fluids in the ORC cycle is so important to achieve high thermal efficiency. In this study, toluene is selected as a working fluid. All needed relations for modeling and simulation of the ORC cycle are provided in (Ding et al., 2018). Also, the main parameters of the Organic Rankin Cycle are shown in Table (3).

Table3. The main parameters for ORC

Main parameter	value
Organic fluid quality at turbine inlet	1
Organic fluid Pressure at turbine inlet	30 (bar)
ORC pump isentropic efficiency (%)	75
ORC turbine isentropic efficiency (%)	80
Exhaust gas temperature	120 (°C)
Organic fluid quality at condenser outlet	0
Organic fluid temperature at condenser outlet	54 (°C)

4. Exergy analysis

Exergy is expressed as the maximum theoretical useful work capability of a system when its state is brought to equilibrium with its surroundings. The results of the exergy analysis presented the location, the source, and the magnitude of thermodynamic inefficiencies in any thermal system. Exergy flow equation for a control volume is expressed as (Rad, Khoshgoftar Manesh, Rosen, Amidpour, & Hamed, 2016):

$$\sum Q \left(1 - \frac{T_0}{T}\right) - W + \sum_{in} m_i e_{in} - \sum_{out} m_{out} e_{out} = E_D \quad (25)$$

Table 4. cost function of the component

Component	Cost function
Air and Fuel compressors	$Z_{AC} = \frac{71.1m_a}{0.9 - \eta_{AC}} \left(\frac{P_{dc}}{P_{suc}}\right) \ln\left(\frac{P_{dc}}{P_{suc}}\right)$
	$Z_{FC} = \frac{71.1m_{fuel}}{0.9 - \eta_{AC}} \left(\frac{P_{dc}}{P_{suc}}\right) \ln\left(\frac{P_{dc}}{P_{suc}}\right)$ (Kotas, T.J., "The exergy method of thermal plant analysis" & Florida, n.d.)
Gas Turbine	$Z_{GT} = (-98.328 \ln(W_{GT}) + 1318.5) \times W_{GT}$ (Shirazi et al., 2012)
Heat Exchangers	$Z_{HX} = 8500 + 46A_{HX}^{0.85}$ (Shirazi et al., 2012)
	$Z_{HX} = 4122 \times \left(\frac{m_g (h_{11} - h_{12}) \times 1000}{18 \times \Delta T_{lm.HX}}\right)^{0.6}$
Heat Exchanger 2	$\Delta T_{lm.HX} = \frac{(T_{11} - T_6) - (T_{12} - T_5)}{\ln \frac{T_{11} - T_6}{T_{12} - T_5}}$ (Kotas, T.J., "The exergy method of thermal plant analysis" & Florida, n.d.)

By ignoring the exergy of nuclear, electrical, and surface tension, kinetic and potential effects, the exergy of a stream is the sum of its physical and chemical exergies:

$$\varepsilon = \varepsilon_{ph} + \varepsilon_{ch} \quad (26)$$

That in this relation, specific flow physical and chemical exergy at any cycle state respectively is given by:

$$\varepsilon_{ph} = h - h_o - T_o (s - s_o) \quad (27)$$

$$\varepsilon_{ch} = \sum x_k \varepsilon_k^{ch} - RT_0 \sum x_k \ln x_k \quad (28)$$

5. Exergoeconomic Analysis

For economic analysis, the capital cost of each component listed in Table (4), will be considered. By using the following relation cost function of each component (in terms of the dollar) can be converted into the cost per unit time (Shirazi et al., 2012).

$$Z_k = \frac{Z_k \times CRF \times \Phi}{N \times 3600} \quad (29)$$

In this relation N represent the annual operating hours of the system, ϕ is the maintenance factor and CRF is Capital Recovery Factor expressed as:

$$CRF = \frac{i(1+i)^n}{(1+i)^n - 1} \quad (30)$$

i and n respectively represent interest rate and system lifetime. In this study, the cost of the fuel specified by 4.57\$/GJ-exergy and the specific cost of the incoming air and water assumed to be zero.

Component	Cost function
After Burner and combustion chamber	$Z_{AB} = \left(\frac{46.08 m_{ab}}{0.995 - \frac{P_9}{P_8}} \right) [1 + \exp(0.018T_9 - 26.4)]$
	(Kotas, T.J., "The exergy method of thermal plant analysis" & Florida, n.d.)
SOFC	$Z_{SOFC} = A_{SOFC} (2.96T_{SOFC} - 1907)$ $Z_{inv} = 10^5 (W_{cell} / 500)^{0.7} \quad (\text{Shirazi et al., 2012})$ $Z_{aux} = 0.1 \times Z_{SOFC}$
Gas turbine	$Z_{GT} = \frac{479.34 \times m_g}{0.92 - \eta_{GT}} \times \ln\left(\frac{P_{dc}}{P_{suc}}\right) [1 + \exp(0.036T_9 - 54.4)]$
	(Kotas, T.J., "The exergy method of thermal plant analysis" & Florida, n.d.)
HRVG and Recuperator	$Z_{re} = 6570 \left(\frac{Q_{re}}{LMTD_{re}} \right)^{0.8} + 2127 m_{of} + 1184.4 m_g^{1.2}$
	(Roy, Samanta, & Ghosh, 2019)
Organic Turbine	$Z_T = 6000 \times W_t^{0.7} \quad (\text{Nazari, Heidarnejad, & Porkhial, 2016})$
Organic Pump	$Z_p = 3540 \times W_p^{0.71} \quad (\text{Nazari et al., 2016})$
Organic Condenser	$Z_C = 1773 \times m_{of} \quad (\text{Nazari et al., 2016})$

6. Advanced Exergy analysis

The advanced exergy analysis considers the effects of components on one another (endogenous/exogenous) and also accounts the extent to which an equipment performance can be improved based on limitation of recent technology (avoidable/unavoidable) as follows (Khoshgoftar Manesh, Navid, Blanco Marigorta, Amidpour, & Hamed, 2013):

$$\dot{E}_{D,k} = \dot{E}_{D,k}^{UN} + \dot{E}_{D,k}^{AV} \quad (31)$$

The unavoidable investment cost ($\dot{Z}_{D,k}^{UN}$)

$$\dot{Z}_k = \dot{Z}_k^{UN} + \dot{Z}_k^{AV} \quad (32)$$

The unavoidable ($\dot{E}_{D,k}^{UN}$) exergy destruction cannot be further reduced due to technological limitations. The avoidable exergy destruction ($\dot{E}_{D,k}^{AV}$) is the difference between total and unavoidable exergy destruction for a component.

The exogenous part of the exergy destruction is the difference between the exergy destruction of the component in the real system and the ideal system. The endogenous/exogenous parts are defined as follows:

$$\dot{E}_{D,k} = \dot{E}_{D,k}^{EN} + \dot{E}_{D,k}^{EX} \quad (33)$$

$$\dot{Z}_k = \dot{Z}_k^{EN} + \dot{Z}_k^{EX} \quad (34)$$

To overcome the limitation of the thermodynamic method to split the exergy destruction, the engineering method is proposed by Kelly et al (Kelly, Tsatsaronis, & Morosuk, 2009). The following relation is applied to find the exogenous/endogenous parts of exergy destruction:

$$\dot{E}_{D,tot} = \dot{E}_{D,k}^{EN} + \dot{E}_{D,k}^{EX} + \dot{E}_{D,others} \quad (35)$$

where $\dot{E}_{D,others}$ is the sum of exergy destruction rates in system components other than that in component k. Referring to Eq. (35) and Fig.2, if the $\dot{E}_{D,others}$ converges to zero, the exogenous exergy destruction rate for k component becomes zero and the endogenous part is calculated.

The avoidable endogenous part of exergy destruction is a variable used in an advanced exergy-based analysis ($\dot{E}_{D,k}^{AV,EN}$, $\dot{Z}_{D,k}^{AV,EN}$, $C_{D,k}^{AV,EN}$). This parameter can be reduced by improving the kth component from the exergetic and economic views.

In addition, avoidable endogenous part of exergy destruction cost is calculated:

$$\dot{C}_{D,k}^{AV,EN} = c_{F,k} \cdot \dot{E}_{D,k}^{AV,EN} \quad (36)$$

7. Results and Discussion

In this study thermodynamic simulation with advanced and conventional exergetic analysis of direct and indirect coupling of five SOFC stacks with GT and ORC cycle has been performed. The verification of SOFC stack results has been done by Ref (Chitsaz et al., 2015) and (Tao, Armstrong, & Virkar, 2019). The results comparison is determined in Table (5) that represented the cell voltage and power density obtained for several values of the current density. As indicated, the calculated values indicate high accuracy between present work and those reported by Tao et al (Tao et al., 2019) and Chitsaz et al (Chitsaz et al., 2015).

The thermodynamic and exergoeconomic analysis at different state points for the hybrid

cycle have been shown in Table (6) and other exergetic and exergoeconomic analysis stream data have been indicated in Table (7).

The thermodynamic analysis showed that for the SOFC-GT combination without using ORC, net power, electrical efficiency, exergetic efficiency, and total efficiency are 11.068MW, 38.98%, 36.69%, and 42.83% respectively. Using ORC, thermal efficiency, net power, electrical efficiency, exergetic efficiency, and total efficiency reach 16.69%, 12.17 MW, 42.84%, 40.34 and 59.53% respectively.

As shown in Fig. 3, the most exergy destruction belongs to CC, SOFC, and AB respectively. Table (7) shows that C_D for HRVG, SOFC, and CC are the highest rank. Further results indicate that the r_k for recuperator is the highest value.

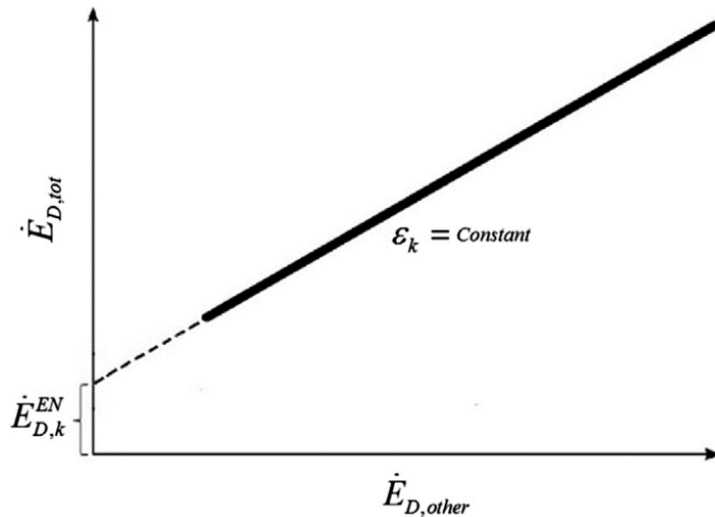


Figure 2. Find the $\dot{E}_{D,k}^{EN}$ by variation of $\dot{E}_{D,others}$ and $\dot{E}_{D,tot}$ Kelly (Kelly et al., 2009)

Table 5. Comparison of the results obtained from this work with those reported by Chitsaz et al. (Chitsaz et al., 2015) and Tao et al (Tao et al., 2019)

	Current Density ($\frac{A}{m^2}$)			Power Density ($\frac{W}{m^2}$)		
	Present work	Chitsaz et al	Tao et al	Present work	Chitsaz et al	Tao et al
2000	0.764	0.790	0.76	0.149	0.158	0.15
3000	0.699	0.711	0.68	0.205	0.216	0.21
4000	0.640	0.644	0.62	0.251	0.253	0.26
5000	0.586	0.560	0.57	0.287	0.288	0.295
6000	0.535	0.510	0.52	0.314	0.300	0.315

Table 6. Mass flow rate, pressure, temperature and exergoeconomic parameters at different state points for hybrid cycle

	Thermodynamic analysis			Exergoeconomical analysis		
	M ($\frac{kg}{s}$)	T (K)	P (kPa)	Ex (kW)	c ($\frac{\$}{GJ}$)	C ($\frac{\$}{s}$)
1	4.21	298.15	100	18.77	0	0
2	4.21	445.5	325.5	566.39	34.4	0.0195
3	4.21	873.9	312.48	1587.6	19.18	0.0305
4	0.24	298.15	100	12825	4.57	0.0556
5	0.24	656.3	325.5	12959	4.87	0.0632
6	0.24	798.9	312.48	13033	4.92	0.064
7	4.00	1273	300	3699.1	20.969	0.0776

	Thermodynamic analysis			Exergoeconomical analysis		
	M ($\frac{kg}{s}$)	T (K)	P (kPa)	Ex (kW)	c ($\frac{\$}{GJ}$)	C ($\frac{\$}{\$}$)
8	0.45	1273	300	2096.8	20.969	0.044
9	0.45	1480	285	4461.8	27.25	0.1216
10	4.45	1237	105	2911.1	27.25	0.0793
11	15.54	298.15	100	73.03	0	0
12	15.54	640.7	1100	5109.8	12.27	0.0627
13	0.32	298.15	2000	17245	4.57	0.074
14	15.86	1450.15	1056	17204	7.96	0.1371
15	15.86	921.5	108	5539.4	7.96	0.441
16	15.86	824.1	104	4171.3	7.96	0.0332
17	15.86	819.6	100	4060.5	7.96	0.0324
19	4.45	393.15	100	58.824	2.72	0.0016
20	7.08	566.2	3000	14124	62.72	0.8859
21	7.08	431.1	16.03	12784	62.72	0.802
22	7.08	411.4	15.26	12709	62.72	0.7972
23	7.08	327.15	14.54	12290	64.86	0.7972
24	7.08	328.6	3307.5	12319	65.05	0.801
25	7.08	345.9	3150	12343	65.37	0.8069
26	20.7	288.15	100	36252	0	0
27	20.7	330.15	100	36376	0	0

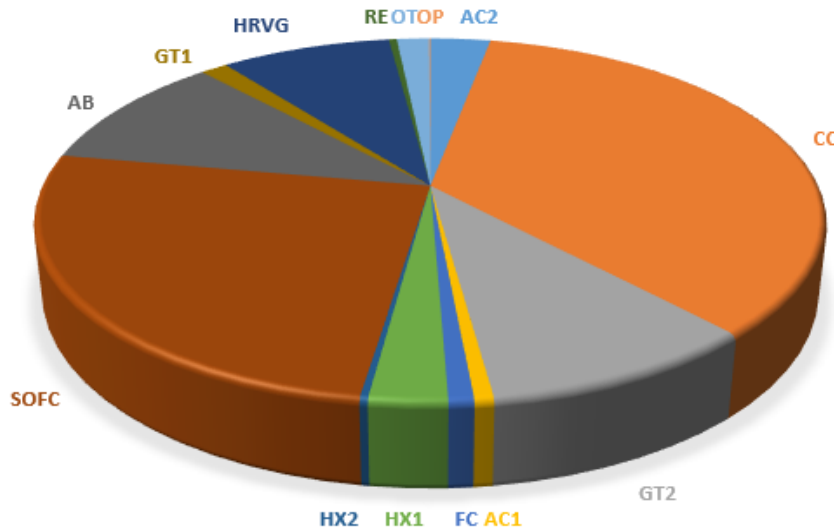


Figure 3. Exergy destruction distribution in SOFC-GT-ORC combined cycle

Table 7. Exeretic and exergoeconomic analysis stream data

Comp.	ϵ (%)	c_r ($\frac{\$}{GJ}$)	c_p ($\frac{\$}{GJ}$)	C_D ($\frac{\$}{\$}$)	Z_T ($\frac{\$}{\$}$)	r_k (%)	f_k (%)
AC2	93.04	11.03	12.45	0.0042	0.003	16.03	41.9
CC	76.96	6.12	7.9	0.0276	0.00018	30.11	0.66
GT2	89.32	7.9	11.03	0.0099	0.022	38.4	68.88
AC1	86.47	30.6	12.4	0.0026	0.00066	16.035	2.45
FC	54.27	30.6	56.5	0.0035	0.000004	84.3	0.11
HX1	76.64	7.9	10.7	0.0028	0.000063	34.75	2.23
HX2	67.34	7.9	12.4	0.000288	0.000046	56.3	13.88
SOFC	77.68	8.67	31.1	0.0283	0.1436	259.47	83.5
AB	76.98	20.9	27.2	0.028	0.000048	29.95	0.17
GT1	89.13	27.2	30.6	0.0046	0.00013	38.4	2.81
HRVG	62.41	27.2	44.3	0.0292	0.0012	62.68	3.9
RE	33.16	62.7	226.3	0.0031	0.00092	260.8	22.7
OT	84.88	62.7	104.8	0.0127	0.0352	67.2	73.5
OP	77.2	104.8	144.1	0.00089	0.00024	37.4	21.11

In exergoeconomic analysis, by considering the value of exergoeconomic factor all components can be classified into three categories. In the first category, the exergoeconomic factor has high value. Understandably, capital costs for these components are very high. For this category, the exergy destruction and relevant cost of exergy destruction must be reduced. In this study, SOFC has the highest value due to its high purchased equipment cost and short lifetime.

In the second category, the exergoeconomic factor has low value and investment cost must to reduce even if the reduction of component efficiency must be accepted. As presented in the results, the lowest value is related to the FC and AB, since the purchased equipment cost of FC is low. In AB, due to chemical reactions significant exergy destruction takes place. Due to low purchased cost and high exergy destruction for AB, cost factor and the exergetic efficiency must be increased by adding the capital costs.

All components that have intermediate values for exergoeconomic factors are in the third category and for improvement these components advanced exergy analysis has been suggested. Tables (8)- (10) and Fig (4)-(6) show advanced analysis data of the SOFC-GT-ORC system.

Table (8) demonstrated the available/unavailable, endogenous/exogenous parts of exergy destruction related to each component. The results of advance exergetic analysis have

been calculated based on Engineering Approach that developed MATLAB code.

The percent of avoidable/ unavoidable and exogenous/endogenous exergy destruction of SOFC-GT-ORC components has been shown in Figure 4.

As shown in Table 7, CC, AB, and HRVG respectively have the highest potential for improvement based on technological limitations. Also, because of exogenous parts of exergy destruction, FC and AC2 have the highest values.

Based on the avoidable cost of exergy destruction (Table 9), HRVG has the maximum potential for improvement. Also, HRVG and SOFC respectively have the highest amount of exogenous cost of exergy destruction.

The percent of avoidable/unavoidable and exogenous/endogenous exergy destruction cost rate of SOFC-GT-ORC of each equipment has been determined in Figure 5.

Table (10) determines the avoidable/unavoidable and exogenous/endogenous parts of capital investment for each component. As indicated in Table (10), the HRVG and HX3 have the maximum amount of avoidable capital investment. Furthermore, the SOFC has a maximum exogenous capital investment rather than other components. The percent of avoidable/unavoidable and exogenous/endogenous capital investment cost of SOFC-GT-ORC components has been demonstrated in Figure 6.

Table 8. Splitting the exergy destruction within the k-th component of SOFC-GT-ORC system.

Component	E_D^{UN} (kW)	E_D^{AV} (kW)	E_D^{EN} (kW)	E_D^{EX} (kW)
AC1	74.07	15.616	62.71	22.95
AC2	350.76	46.22	270.46	106.54
FC	61.07	33.11	79.48	33.05
HX1	258.99	70.47	261.14	85.84
HX2	24.38	10.73	27.37	8.82
CC	3467.97	1023.81	3894.26	611.94
AB	1026.99	335.13	1143.19	190.91
SOFC	2535.55	443.59	2623.03	641.07
GT2	1113.28	134.98	1065.55	180.85
GT1	150.21	15.54	147.07	21.45
HRVG	669.22	324.47	808.08	264.21
RE	16.46	18.49	38.86	10.79
OT	171.94	18.57	154.44	48.13
OP	6.55	1.047	6.55	1.94

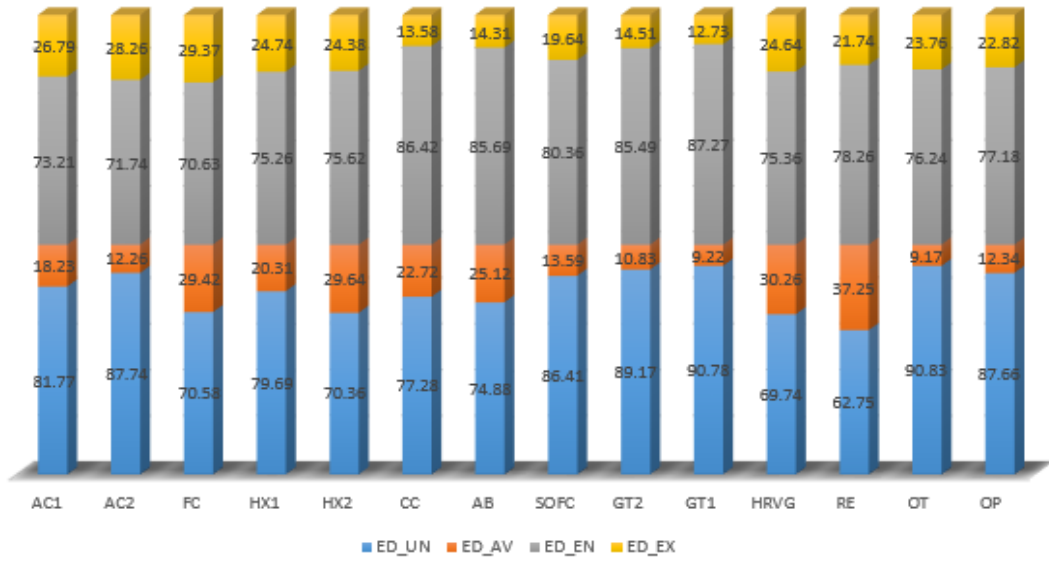


Figure 4. Distribution of avoidable/unavoidable and exogenous/endogenous Exergy Destruction of SOFC-GT-ORC components

Table 9. Splitting the exergy destruction cost rate within the k-th component of the SOFC-GT-ORC system.

Component	C_D^{UN} (\$/s)	C_D^{AV} (\$/s)	C_D^{EN} (\$/s)	C_D^{EX} (\$/s)
AC1	0.00212	0.00048	0.0018	0.00077
AC2	0.00364	0.00055	0.0029	0.0013
FC	0.00264	0.00086	0.0024	0.0011
HX1	0.00219	0.00061	0.0021	0.00069
HX2	0.00021	7.85E-05	0.0002	7.38E-05
CC	0.01676	0.0108	0.0235	0.00404
AB	0.01893	0.0091	0.023	0.0049
SOFC	0.02273	0.0056	0.022	0.0061
GT2	0.00821	0.0017	0.0082	0.0017
GT1	0.00383	0.00077	0.0039	0.00071
HRVG	0.0192	0.01	0.021	0.0078
RE	0.0018	0.0013	0.0025	0.00059
OT	0.1114	0.0016	0.0095	0.0031
OP	0.00078	0.00011	0.00068	0.00021

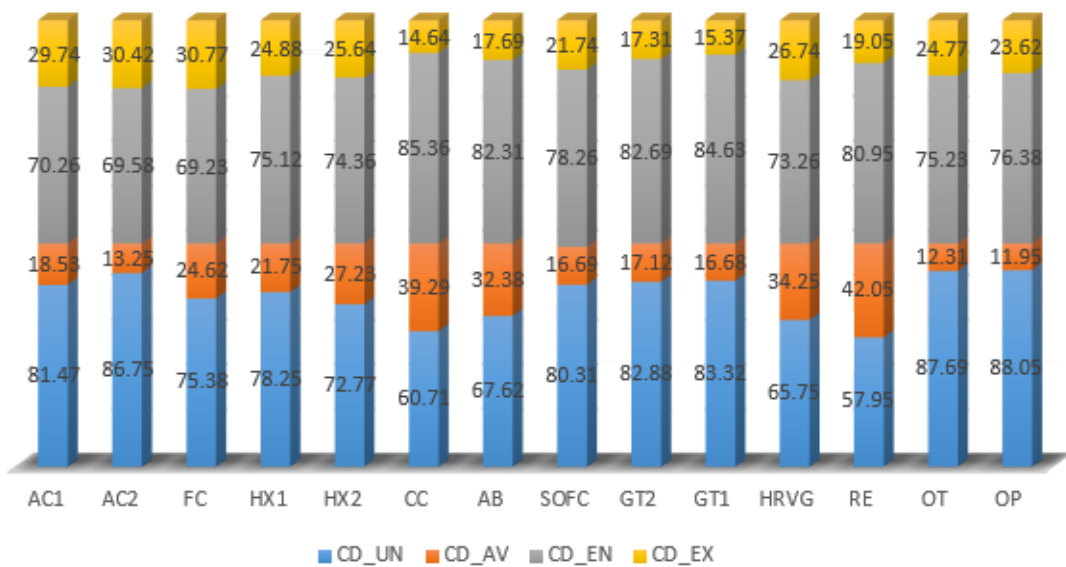
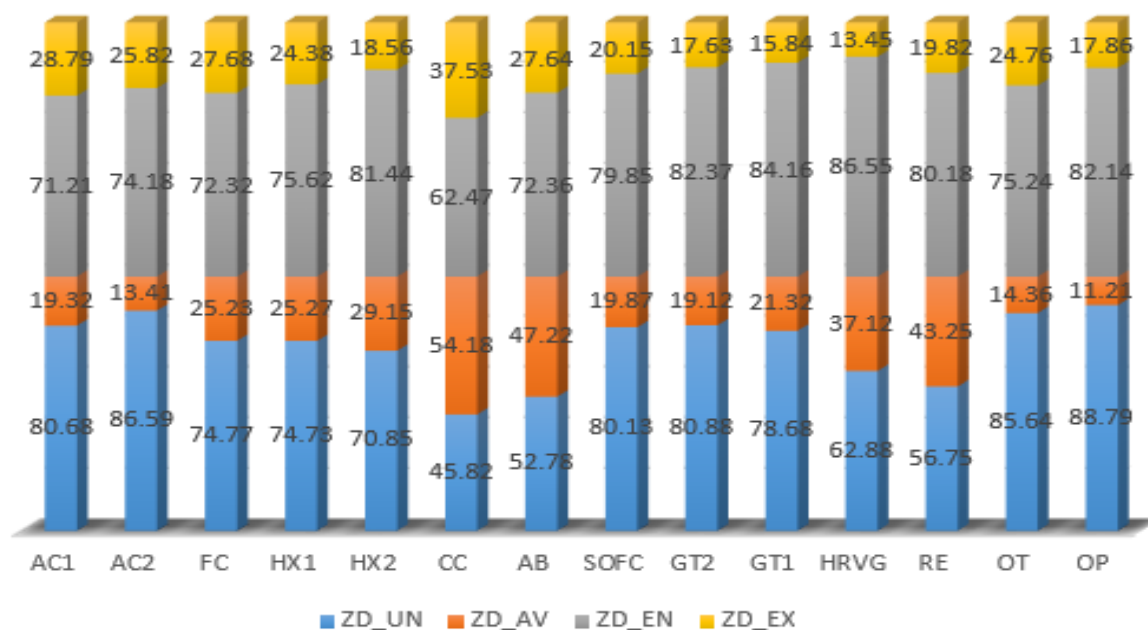


Figure 5. The percent of avoidable/unavoidable and exogenous/endogenous exergy destruction cost rate of SOFC-GT-ORC components

Table 10. Splitting the capital investment cost within the k-th component of the hybridSOFC-GT-ORC system.

Component	Z_D^{UN} (\$/s)	Z_D^{AV} (\$/s)	Z_D^{EN} (\$/s)	Z_D^{EX} (\$/s)
AC1	5.32E-05	1.28E-05	4.7E-05	1.90E-05
AC2	2.60E-03	4.02E-04	2.23E-03	7.75E-04
FC	2.85E-06	9.61E-07	2.76E-06	1.05E-06
HX1	4.72E-05	1.60E-05	4.77E-05	1.54E-05
HX2	3.29E-05	1.36E-05	3.79E-05	8.63E-06
CC	8.43E-05	9.97E-05	1.15E-04	6.91E-05
AB	2.54E-05	2.27E-05	3.48E-05	1.33E-05
SOFC	1.15E-01	2.85E-02	1.15E-01	2.89E-02
GT2	1.78E-02	4.21E-03	1.81E-02	3.88E-03
GT1	1.04E-04	2.83E-05	1.12E-04	2.10E-05
HRVG	7.55E-04	4.45E-04	1.04E-03	1.61E-04
RE	5.20E-04	3.96E-04	7.34E-04	1.81E-04
OT	3.01E-02	5.05E-03	2.65E-02	8.72E-03
OP	2.12E-04	2.67E-05	1.96E-04	4.26E-05

**Figure 6.** Distribution of avoidable/unavoidable and exogenous/endogenous Exergy Destruction Cost Rates ORC components

8. Conclusion

In this paper, a novel integrated SOFC-GT-ORC has been proposed. In this regard, thermodynamic simulation of base and novel cycle has been done by developed Matlab code to compare the performance of base and integrated cases. In addition, conventional and advanced exergetic and exergoeconomic analysis have been performed. Energetic, exergetic, exergoeconomic, endogenous/exogenous, avoidable/unavoidable parts of exergy destruction have been calculated and evaluated by developed code.

Results determine that the net power and overall cycle efficiency of the integrated cycle are increased by 1.1 MW and 7.7 % respectively rather initial base case. Also, exergy efficiency is 40.95%, for the proposed

system and 37.3% for the initial basic configuration. Furthermore, exergoeconomic main parameters and advanced exergetic and exergoeconomic analysis have been calculated and discussed.

The suggestion for improvements of each component based on all performed analyses has been discussed.

In the future study, the conventional and advanced exergoenvironmental analysis based on Life Cycle Assessment (LCA) can be investigated. Also, using different organic fluids can be examined and evaluated. In addition, the optimal design of an integrated cycle based on exergetic and exergoeconomic analysis can be considered.

References

- Ahmadi, R., Pourfatemi, S. M., Ghaffari, S., Muhammad, S., & Ghaffari, S. (2017). Exergoeconomic optimization of hybrid system of GT, SOFC and MED implementing genetic algorithm. *Desalination*, *411*, 76–88. <https://doi.org/10.1016/j.desal.2017.02.013>
- Akkaya, A. V., Sahin, B., Erdem, H. H., Volkan, A., Sahin, B., & Huseyin, H. (2008). An analysis of SOFC/GT CHP system based on exergetic performance criteria. *International Journal of Hydrogen Energy*, *33*(10), 2566–2577. <https://doi.org/10.1016/j.ijhydene.2008.03.013>
- Bavarsad, P. G. (2007). Energy and exergy analysis of internal reforming solid oxide fuel cell–gas turbine hybrid system. *International Journal of Hydrogen Energy*, *32*(17), 4591–4599. <https://doi.org/10.1016/j.ijhydene.2007.08.004>
- Chan, S. H., Low, C. F., & Ding, O. L. (2002). Energy and exergy analysis of simple solid-oxide fuel-cell power systems. *Journal of Power Sources*, *103*(2), 188–200.
- Cheddie, D. F., & Murray, R. (2010a). Thermo-economic modeling of a solid oxide fuel cell/gas turbine power plant with semi-direct coupling and anode recycling. *International Journal of Hydrogen Energy*, *35*(20), 11208–11215. <https://doi.org/10.1016/j.ijhydene.2010.07.082>
- Cheddie, D. F., & Murray, R. (2010b). Thermo-economic modeling of an indirectly coupled solid oxide fuel cell/gas turbine hybrid power plant. *Journal of Power Sources*, *195*(24), 8134–8140. <https://doi.org/10.1016/j.jpowsour.2010.07.012>
- Chitsaz, A., Mahmoudi, S. M. S., & Rosen, M. A. (2015). Greenhouse gas emission and exergy analyses of an integrated trigeneration system driven by a solid oxide fuel cell. *Applied Thermal Engineering*, *86*, 81–90. <https://doi.org/10.1016/j.applthermaleng.2015.04.040>
- Choudhury, A., Chandra, H., & Arora, A. (2013). Application of solid oxide fuel cell technology for power generation—A review. *Renewable and Sustainable Energy Reviews*, *20*, 430–442. <https://doi.org/10.1016/j.rser.2012.11.031>
- Ding, Y., Liu, C., Zhang, C., Xu, X., Li, Q., & Mao, L. (2018). Exergoenvironmental model of Organic Rankine Cycle system including the manufacture and leakage of working fluid. *Energy*, *145*, 52–64. <https://doi.org/10.1016/j.energy.2017.12.123>
- Eveloy, V., Karunkeyoon, W., Rodgers, P., & Al Alili, A. (2016). Energy, exergy and economic analysis of an integrated solid oxide fuel cell–gas turbine–organic Rankine power generation system. *International Journal of Hydrogen Energy*, *41*(31), 13843–13858. <https://doi.org/10.1016/j.ijhydene.2016.01.146>
- Eveloy, V., Rodgers, P., & Qiu, L. (2016). Integration of an atmospheric solid oxide fuel cell - gas turbine system with reverse osmosis for distributed seawater desalination in a process facility. *Energy Conversion and Management*, *126*, 944–959. <https://doi.org/10.1016/j.enconman.2016.08.026>
- Fallah, M., Mahmoudi, S. M. S., & Yari, M. (2018). A comparative advanced exergy analysis for a solid oxide fuel cell using the engineering and modified hybrid methods. *Energy Conversion and Management*, *168*(8), 576–587. <https://doi.org/10.1016/j.enconman.2018.04.114>
- Ghorbani, B., Hamed, M.-H., & Amidpour, M. (2016). Exergoeconomic Evaluation of an Integrated Nitrogen Rejection Unit with LNG and NGL Co-Production Processes Based on the MFC and Absorption Refrigeration Systems. *Gas Processing*, *4*(1), 1–28. <https://doi.org/10.22108/gpj.2016.20410>
- Ghorbani, B., Mehrpooya, M., & Mousavi, S. (2019). Hybrid molten carbonate fuel cell power plant and multiple-effect desalination system. *Journal of Cleaner Production*, *220*. <https://doi.org/10.1016/j.jclepro.2019.02.215>
- Ghorbani, B., Shirmohammadi, R., Mehrpooya, M., & Mafi, M. (2018). Applying an integrated trigeneration incorporating hybrid energy systems for natural gas

- liquefaction. *Energy*, 149, 848–864. <https://doi.org/https://doi.org/10.1016/j.energy.2018.02.093>
- Haseli, Y., Dincer, I., & Naterer, G. F. (2008). Thermodynamic modeling of a gas turbine cycle combined with a solid oxide fuel cell. *International Journal of Hydrogen Energy*, 33(20), 5811–5822. <https://doi.org/10.1016/j.ijhydene.2008.05.036>
- Kelly, S., Tsatsaronis, G., & Morosuk, T. (2009). Advanced exergetic analysis: Approaches for splitting the exergy destruction into endogenous and exogenous parts. *Energy*, 34(3), 384–391. <https://doi.org/10.1016/j.energy.2008.12.007>
- Khoshgoftar Manesh, M. H., Navid, P., Blanco Marigorta, A. M., Amidpour, M., & Hamed, M. H. (2013). New procedure for optimal design and evaluation of cogeneration system based on advanced exergoeconomic and exergoenvironmental analyses. *Energy*, 59. <https://doi.org/10.1016/j.energy.2013.06.017>
- Kotas, T.J., “The exergy method of thermal plant analysis,” K. P. C., & Florida, 1995. (n.d.).
- McPhail, S. J., Aarva, A., Devianto, H., Bove, R., & Moreno, A. (2011). SOFC and MCFC: Commonalities and opportunities for integrated research. *International Journal of Hydrogen Energy*, 36(16), 10337–10345. <https://doi.org/https://doi.org/10.1016/j.ijhydene.2010.09.071>
- Motahar, S., & Alemrajabi, A. A. (2009). Exergy based performance analysis of a solid oxide fuel cell and steam injected gas turbine hybrid power system. *International Journal of Hydrogen Energy*, 34(5), 2396–2407. <https://doi.org/10.1016/j.ijhydene.2008.12.065>
- Motahar, S., Alemrajabi, A. A., Seidler, S., Henke, M., Kallo, J., Bessler, W. G., ... Friedrich, K. A. (2009). Exergy based performance analysis of a solid oxide fuel cell and steam injected gas turbine hybrid power system. *International Journal of Hydrogen Energy*, 34(5), 2396–2407. <https://doi.org/10.1016/j.ijhydene.2008.12.065>
- Nazari, N., Heidarnejad, P., & Porkhial, S. (2016). Multi-objective optimization of a combined steam-organic Rankine cycle based on exergy and exergoeconomic analysis for waste heat recovery application. *Energy Conversion and Management*, 127, 366–379. <https://doi.org/10.1016/j.enconman.2016.09.022>
- Ni, M., Leung, D. Y. C., & Leung, M. K. H. (2009). Electrochemical modeling and parametric study of methane fed solid oxide fuel cells. *Energy Conversion and Management*, 50(2), 268–278. <https://doi.org/10.1016/j.enconman.2008.09.028>
- Pirkandi, J., Ghassemi, M., Hamed, M. H., & Mohammadi, R. (2012). Electrochemical and thermodynamic modeling of a CHP system using tubular solid oxide fuel cell (SOFC-CHP). *Journal of Cleaner Production*, 29, 151–162. <https://doi.org/10.1016/j.jclepro.2012.01.038>
- Pirkandi, J., Mahmoodi, M., & Ommian, M. (2017). An optimal configuration for a solid oxide fuel cell-gas turbine (SOFC-GT) hybrid system based on thermo-economic modelling. *Journal of Cleaner Production*, 144, 375–386. <https://doi.org/10.1016/j.jclepro.2017.01.019>
- Quoilin, S., Van Den Broek, M., Declaye, S., Dewallef, P., & Lemort, V. (2013). Techno-economic survey of Organic Rankine Cycle (ORC) systems. *Renewable and Sustainable Energy Reviews*, 22, 168–186.
- Rad, M. P., Khoshgoftar Manesh, M. H., Rosen, M. A., Amidpour, M., & Hamed, M. H. (2016). New procedure for design and exergoeconomic optimization of site utility system considering reliability. *Applied Thermal Engineering*, 94. <https://doi.org/10.1016/j.applthermaleng.2015.10.091>
- Ramezani, M.-A., Amidpour, M., Najafi, M., & Abbaspour, M. (2015). A Study on Performance of Solid Oxide Fuel Cell-Stirling Engine Cycle Combined System- Part I: SOFC Simulation by Programming in Matlab and Modeling in Hysys. *Gas Processing*, 3(2), 55–70. <https://doi.org/10.22108/gpj.2015.20406>
- Rangel-hernández, H., Hugo, V., Juan, M., Elizalde-Blancas, F., Rangel-Hernández, V. H., Niño-Avendaño, A. M., ...

- Elizalde-Blancas, F. (2018). Advanced Exergy Analysis of an Integrated SOFC-Adsorption Refrigeration Power System. *Application of Exergy*, 65. <https://doi.org/10.5772/intechopen.74201>
- Roy, D., Samanta, S., & Ghosh, S. (2019). Techno-economic and environmental analyses of a biomass based system employing solid oxide fuel cell, externally fired gas turbine and organic Rankine cycle. *Journal of Cleaner Production*, 225, 36–57.
- Sghaier, S. F., Khir, T., & Brahim, A. Ben. (2018). Energetic and exergetic parametric study of a SOFC-GT hybrid power plant. *International Journal of Hydrogen Energy*, 43(6), 3542–3554. <https://doi.org/10.1016/j.ijhydene.2017.08.216>
- Shirazi, A., Aminyavari, M., Najafi, B., Rinaldi, F., & Razaghi, M. (2012). Thermal–economic–environmental analysis and multi-objective optimization of an internal-reforming solid oxide fuel cell–gas turbine hybrid system. *International Journal of Hydrogen Energy*, 37(24), 19111–19124.
- Tao, G., Armstrong, T., & Virkar, A. (2019). *Intermediate Temperature Solid Oxide Fuel Cell Intermediate Temperature Solid Oxide Fuel Cell (IT - -SOFC) Research and Development Activities MSRI at MSRI*.
- Wang, J., Yan, Z., Ma, S., & Dai, Y. (2012). Thermodynamic analysis of an integrated power generation system driven by solid oxide fuel cell. *International Journal of Hydrogen Energy*, 37(3), 2535–2545. <https://doi.org/10.1016/j.ijhydene.2011.10.079>
- Zhang, X., Chan, S. H., Li, G., Ho, H. K., Li, J., & Feng, Z. (2010). A review of integration strategies for solid oxide fuel cells. *Journal of Power Sources*, 195(3), 685–702.

